Spacetime Curvature and Localized Energy Density Emerge from Quantum Energy Teleportation Protocols

Daniel S. Zachary

[1] Advanced Academic Program, Krieger School of Arts and Sciences, Johns Hopkins University, Washington DC, 555 Pennsylvania Avenue, NW, 20001, USA

July 24, 2025

We propose a theoretical framework in which spacetime curvature and localized energy density emerge from modulations of vacuum entanglement structure. Building upon quantum energy teleportation (QET) protocols and the entanglement-geometry correspondence, we introduce an operational mechanism by which local measurements can induce energy redistribution across spacelike-separated regions. This mechanism does not involve classical signal propagation and remains consistent with causality and quantum energy inequalities. We formalize this hypothesis through an effective entanglement stress-energy tensor and derive its implications for geometry, energy flow, and negative energy densities. Experimental signatures include curvature shifts detectable by atom interferometers, clock desynchronization in optical networks, and vacuum pressure changes in Casimir systems. We identify feasible experimental platforms and outline protocols to test this proposal within current or near-future precision measurement technologies.

1 Introduction: Entanglement as a Source of Energy and Geometry

The vacuum is not an inert but a profoundly entangled quantum state, as shown in quantum field theory (QFT) [1, 2]. Spatially separated regions of the vacuum exhibit nontrivial correlations, leading to phenomena such as the area-law scaling of entanglement entropy and the failure of reduced density matrices to factorize across spacelike separations. These entanglement features are not merely mathematical artifacts—they encode physically meaningful structure. Recent developments indicate that vacuum entanglement can give rise to observable effects, including local energy redistributions [5, 9, 10] and even contributions to spacetime geometry [3, 17, 18].

In this paper, we propose the *Quantum Nexus Initiated via Vacuum Entanglement with Spacetime Emergence* (Q-UNIVERSE) hypothesis, as a framework in which energy and curvature are operational consequences of entanglement activation. Building on our earlier proposal [6] (Quantum Interferometric Extraction, QIX), we now extend the conceptual and experimental reach of this idea by providing a generalized mechanism, new observational criteria, and a modular entanglement stress tensor.

Daniel S. Zachary: d.s.zachary@jhu.edu

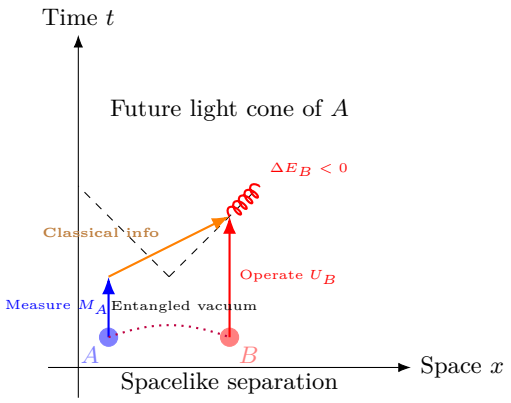

Figure 1: Causal structure of QUINT thread activation. A measurement at region A perturbs the entangled vacuum. Classical information is sent to region B, where a local operation causes an energy redistribution consistent with QEIs, appearing as a negative energy shift (indicated by the coil decoration representing localized energy flux). No signal exceeds the light cone.

1.1 From Quantum Energy Teleportation to Entanglement Stress

The Quantum Energy Teleportation (QET) protocol [5, 11, 12] reveals that local operations and classical communication (LOCC) on entangled vacuum states can result in net energy transfer without violating causality. This operational framework decouples the appearance of energy from conventional local sources, suggesting that energy can emerge from informational constraints imposed on the vacuum. The causal sequence of such a QET/QUINT operation is illustrated in Fig. 1, which shows how local measurements and classical communication lead to energy redistribution without superluminal signaling.

We reinterpret these findings as indicative of a broader principle: energy fluxes in quantum systems arise from conditional manipulation of entanglement. This gives rise to the postulate that classical energy density $T_{\mu\nu}$ is incomplete unless supplemented by an *entanglement stress-energy tensor*, $\mathcal{T}^{(\mathrm{ent})}_{\mu\nu}$, encoding the geometric response to entanglement restructuring:

$$G_{\mu\nu} + \Lambda g_{\mu\nu} = 8\pi G \left(\langle T_{\mu\nu} \rangle + \mathcal{T}^{(\mathrm{ent})}_{\mu\nu} \right). \tag{1}$$

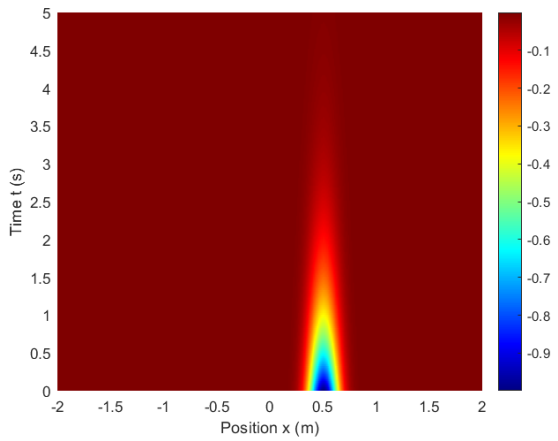

Figure 2: Spatial profile of the energy density shift $\langle T_{00}(x,t) \rangle$ at time $t = t_A + \Delta t + \sigma$, showing a localized negative energy dip near detector B at $x = +\frac{d}{2}$. The dip is bounded and consistent with QEIs, illustrating the nonlocal yet causal nature of the protocol.

As shown in Fig. 2, the negative energy dip is localized near detector B and respects the causal constraints imposed by the QET/QUINT protocol. This illustrates how conditional operations on the entangled vacuum can generate measurable energy shifts without violating causality.

Example spatial profiles of the entanglement-induced stress-energy are shown in Figs. B2–5, where Gaussian models (heat maps) and schematic modular flow diagrams illustrate how entanglement restructuring can generate effective curvature contributions.

Figure 5 shows the full spacetime evolution of the energy density $\langle T_{00}(x,t) \rangle$ following a QET measurement at detector A. The negative energy feature propagates causally and decays in accordance with quantum energy inequality constraints, remaining strictly within A's future light cone.

1.2 Limitations of Holography and Motivation for Flat-Spacetime Models

The Ryu–Takayanagi proposal [13, 20] and ER=EPR conjecture [4, 14] link geometry and entanglement in the context of AdS/CFT duality. However, these approaches are typically confined to asymptotically anti-de Sitter spaces and often depend on boundary dualities not present in our universe. By contrast, the Q-UNIVERSE framework proposes that entanglement-induced energy and curvature can be observed in flat or weakly curved spacetime through localized experimental protocols, circumventing the need for a full theory of quantum gravity. Inspired by tensor network models and relative entropy techniques [15, 18], Q-UNIVERSE suggests that curvature may emerge from entanglement gradients, heuristically expressed as

$$\delta R \sim \nabla^2 S_{\mathrm{ent}}. \tag{2}$$

This formulation invites direct experimental investigation of entanglement–curvature relationships in laboratory systems.

Table 3 summarizes how proposed observables in experimental platforms correspond to modular Hamiltonians and entanglement quantities in the Q-UNIVERSE framework.

1.3 What is New in This Work

First, we formalize the entanglement stress-energy tensor and define its role in curvature response, extending the scope of semiclassical Einstein equations.

Second, we propose operational protocols—based on interferometry, optical clocks, Casimir cavities, and squeezed vacuum experiments—to test the presence of energy or curvature redistribution induced by vacuum entanglement activation. The main classes of feasible probes are organized in Table 3, which lists representative experimental systems and the observables relevant for detecting entanglement-induced energy redistribution.

Third, we define and distinguish *QUINT threads*: operational, non-geometric conduits that mediate entanglement-conditioned energy redistribution across spacelike separations. These are distinct from ER=EPR wormholes by virtue of their testability and flat-spacetime implementation. Table C1 summarizes the proposed null-test protocols, highlighting the role of entanglement by contrasting outcomes with separable or classically correlated states.

Finally, we outline how the Q-UNIVERSE hypothesis provides a novel reinterpretation of cosmological dark energy, curvature fluctuations, and information-theoretic formulations of gravitational dynamics.

2 Postulates and Formal Framework

The Q-UNIVERSE hypothesis begins with a reinterpretation of the quantum vacuum—not as a passive background, but as an actively entangled medium capable of informational and energetic redistribution. From this viewpoint, the apparent emptiness of spacetime hides a vast resource of correlations that, when perturbed, can give rise to energy and even curvature without local classical excitation.

First, we postulate that the vacuum state $|\Omega\rangle$ is a physically real, spatially extended quantum object that encodes entanglement between all spacetime regions. This structure is not simply an artifact of Hilbert space factorization, but corresponds to measurable, causal features of the field. In quantum field theory, this claim is supported by the Reeh–Schlieder theorem, which asserts that the vacuum is cyclic and separating for the field algebra in any open region, implying that local operations on the vacuum can affect arbitrarily distant regions of space [25].

Second, energy is regarded not as a primitive observable, but as an emergent quantity defined relative to local perturbations in the entanglement structure of the vacuum. This framework draws on results from quantum energy teleportation (QET), in which a local measurement in one region, accompanied by a classical signal and a conditional operation in another, can redistribute the field's local energy density without transporting any classical energy [5]. The energy extracted or depleted in this process is not created ex nihilo, but reorganized from pre-existing quantum correlations.

Third, we hypothesize that spacetime geometry itself responds to changes in the vacuum's entanglement structure. This extends earlier proposals in AdS/CFT duality, where boundary entanglement entropy is associated with bulk geometry through the Ryu–Takayanagi relation [20]. However, Q-UNIVERSE generalizes this logic beyond asymptotically AdS spaces and proposes a direct, local relation in flat or weakly curved spacetimes.

To capture this relation, we introduce an *entanglement stress-energy tensor*, $\mathcal{T}^{(\mathrm{ent})}_{\mu\nu}$, which modifies the Einstein field equations:

$$G_{\mu\nu} + \Lambda g_{\mu\nu} = 8\pi G \left(\langle T_{\mu\nu} \rangle + \mathcal{T}^{(\mathrm{ent})}_{\mu\nu} \right), \tag{3}$$

where $\langle T_{\mu\nu} \rangle$ is the usual renormalized stress-energy tensor and $\mathcal{T}^{(\mathrm{ent})}_{\mu\nu}$ encodes purely entanglement-induced curvature. The tensor is defined by variation of an entropy-action functional with respect to the metric,

$$\mathcal{T}^{(\mathrm{ent})}_{\mu\nu}(x) := \frac{2}{\sqrt{-g}} \frac{\delta S_{\mathrm{ent}}}{\delta g^{\mu\nu}(x)}, \tag{4}$$

where S_{ent} represents a generalized entropy functional, such as entanglement entropy across causal surfaces. Its variation quantifies the response of geometry to entanglement restructuring, analogous to the derivation of the classical matter stress tensor from an action.

Next, we introduce the notion of *QUINT threads*—nonlocal informational pathways within the vacuum that mediate energy redistribution (Fig. 3). These threads are operationally defined: they are not ontologically pre-existing conduits like wormholes, but become real through the activation of vacuum entanglement by localized quantum measurements and conditional operations. Their presence is diagnosed via changes in local energy expectation values, clock rates, or curvature perturbations in distant but entangled regions [44]. Unlike wormholes, QUINT threads have no geometric embedding; they exist only as operational channels revealed by measurement-conditioned redistribution.

Figure 3 illustrates the conceptual distinction: (a) QUINT threads are operational entanglement links with observable consequences such as energy extraction or clock drift, without requiring any geometric embedding; (b) ER=EPR wormholes identify entanglement with a non-traversable spacetime bridge, which is inferred rather than directly measurable.

Finally, this framework respects constraints from quantum energy inequalities (QEIs), which forbid arbitrarily large or sustained negative energy densities. Any redistribution via QUINT threads must obey bounds of the form

$$\int_{-\infty}^{\infty} dt\, f^2(t)\, \langle T_{00}(t, \vec{x}) \rangle \geq -\frac{C}{\tau^4}, \tag{5}$$

where $f(t)$ is a smooth sampling function of width τ and C is a model-dependent constant [26]. These bounds are automatically respected in QET and, by construction, in Q-UNIVERSE.

Altogether, the framework rests on the assertion that the structure of vacuum entanglement is not only observable but energetically consequential. Energy may therefore be regarded as a kind of "entanglement bookkeeping"—a physical response to how correlations are conditioned or collapsed. Spacetime curvature becomes a response function to entanglement variation, not merely to classical stress-energy.

2.1 Ontological Status of the Vacuum

The vacuum in quantum field theory is not an empty background, but a dynamically entangled substrate capable of transmitting correlations and fluctuations. In our approach, this entangled vacuum is essential for the mediation of energy–information exchange via the QET protocol. This view aligns with a broader shift in modern physics toward treating the vacuum as a physical medium with real ontological content. Historical precursors include the Dirac sea, which modeled the vacuum as a filled continuum of negative energy states, and stochastic electrodynamics, which treated vacuum fluctuations as physically operative noise. In our context, the entangled vacuum provides the conduit for energy extraction at spacelike separation, reinforcing its interpretation as a nontrivial component of the quantum spacetime fabric. These interpretations converge with recent developments in holography and spacetime emergence, where vacuum entanglement structure is foundational to geometry itself.

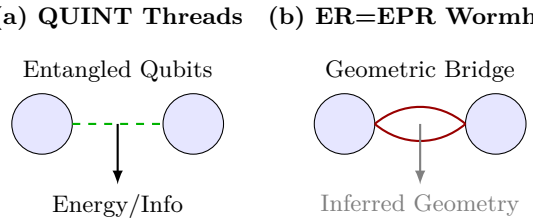

Figure 3: Comparison of entanglement-mediated connections. (a) QUINT threads are operational entanglement links with observable consequences such as energy extraction or clock drift, without geometric embedding. (b) ER=EPR identifies entanglement with a non-traversable wormhole in spacetime geometry.

2.2 Vacuum Correlation Examples

Empirical evidence for vacuum entanglement arises in several well-studied phenomena. The Unruh effect shows that an accelerated observer detects a thermal bath of particles in what inertial observers describe as vacuum, revealing observer-dependent excitations tied to vacuum correlations [29]. The Casimir effect manifests as an attractive force between conducting plates due to altered vacuum field modes, a direct consequence of vacuum fluctuations [30]. Experimental realizations have also confirmed vacuum-induced entanglement between spatially separated detectors [31], underscoring that vacuum entanglement is not a theoretical artifact but a measurable resource. These examples substantiate the interpretation of the vacuum as an active, entangled substrate underlying quantum fields.

Figure 4 illustrates conceptual models of the vacuum: panel (a) shows energy–momentum dispersion for the Dirac plus stochastic vacuum, while panel (b) depicts an entangled vacuum configuration in position space with linked pairs of localized states.

2.3 Energy as Emergent

Traditional physics treats energy as a fundamental conserved quantity tied to time-translation symmetry via Noether's theorem [28]. However, developments in quantum information and holography suggest a different view: energy may be a derived or emergent property arising from entanglement structure. Local energy densities such as $\langle T_{00}(x)\rangle$ are then bookkeeping devices summarizing how correlations are distributed.

This aligns with QET, where local operations and classical communication allow energy to be extracted from the vacuum without net flux. Energy becomes relational—what one observer extracts depends on prior correlations. Unlike Noetherian invariance, which presupposes global spacetime symmetries, QET highlights the operational role of entanglement in generating effective energy flow. These insights echo broader themes in quantum gravity, where gravitational dynamics may emerge from entanglement entropy across causal surfaces. In Q-UNIVERSE, energy conservation is not abandoned but reinterpreted as a consistency condition on entanglement dynamics, bounded by QEIs.

These perspectives dovetail with the holographic principle and tensor-network models, where spatial connectivity arises from entanglement structure [35]. They also complement thermodynamic derivations of gravity such as Jacobson's entanglement equilibrium and Padmanabhan's equipartition model, both of which frame spacetime geometry as a coarse-grained statistical result of underlying entanglement dynamics.

3 Entanglement Geometry in Flat Spacetime

The preceding sections introduced the notion that vacuum entanglement underlies emergent energy and geometry. In this section, we formalize the theoretical framework by presenting core postulates, key equations, and derivations that underpin the Q-UNIVERSE hypothesis. Our aim is to clarify the operational and mathematical structure from which the entanglement stress-energy tensor, $\mathcal{T}_{\mu\nu}^{(\mathrm{ent})}$, emerges as a derived, physically meaningful quantity.

3.1 Postulates of the Q-UNIVERSE Hypothesis

The framework begins with four foundational postulates: First, the vacuum state $|\Omega\rangle$ encodes a global network of quantum correlations, realized as entanglement spanning all spacetime regions. This entanglement is not merely a formal artifact, but a physically meaningful structure that allows local operations to condition distant subsystems, as implied by the Reeh–Schlieder theorem [25]. The vacuum thus acts as a nontrivial, spatially extended resource capable of mediating informational and energetic effects across spacelike separations.

Second, local operations on one region, combined with classical communication, can activate energy redistributions at spacelike separated locations without violating causality, as established by quantum energy teleportation (QET) protocols [5]. Third, these entanglement-induced energy redistributions manifest as modifications to the classical stress-energy content, encoded in an entanglement stress tensor $\mathcal{T}_{\mu\nu}^{(\mathrm{ent})}$. Finally, the response of spacetime geometry to both classical and entanglement stress-energy satisfies a generalized Einstein field equation, previously introduced in Eq. (3), where the total source includes both the renormalized expectation value $\langle T_{\mu\nu}\rangle$ and the entanglement-induced contribution $\mathcal{T}_{\mu\nu}^{(\mathrm{ent})}$.

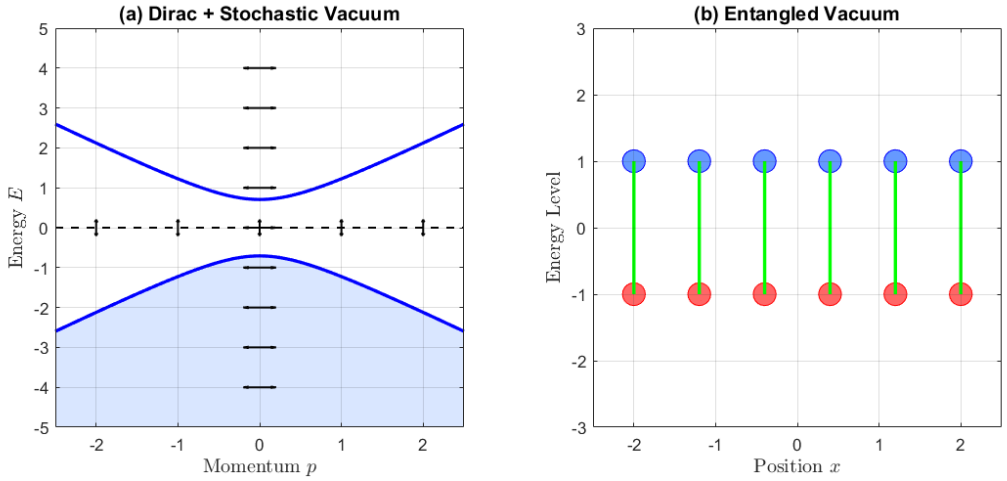

Figure 4: Vacuum concept visualization. **(a)** Energy–momentum dispersion illustrating the Dirac plus stochastic vacuum. The hyperbolic curve (blue) represents the negative-energy Dirac sea with momentum p on the horizontal axis and energy E on the vertical axis. The zero-energy level is marked by a dashed horizontal line at $E = 0$. Bidirectional arrows indicate fluctuations around this baseline. The shaded region beneath the hyperbola highlights occupied negative-energy states. **(b)** Schematic of an entangled vacuum configuration in position space. Two rows of colored markers represent entangled state pairs localized at positions x (red and blue dots), connected by green lines symbolizing entanglement links. Energy levels of these pairs are symmetric about zero, positioned at $E = \pm 1$, emphasizing the vacuum's entangled nature with zero net energy offset.

3.2 Entanglement-Induced Curvature and Energy Redistribution

The entanglement stress-energy tensor is constructed via variation of an entropy-action functional $S_{\text{ent}}[g]$ with respect to the metric, analogous to the derivation of the classical matter stress tensor from a matter action. The functional S_{ent} encodes the information-theoretic structure of the vacuum and its sensitivity to local geometric variations, allowing the resulting tensor $\mathcal{T}^{(\text{ent})}_{\mu\nu}$ to describe entanglement-induced curvature contributions beyond those captured by conventional energy–momentum sources [32].

Building on QET protocols, this formalism gives operational meaning to *QUINT threads*—non-geometric, informational conduits within the entangled vacuum. These threads mediate energy redistribution without classical carriers or direct energy flux. A local measurement followed by a conditional operation at a distant location produces a net energy shift

$$\Delta E_B = \text{Tr}\left(H_B U_B \rho_B U_B^\dagger\right) - \text{Tr}\left(H_B \rho_B\right), \qquad (6)$$

despite no energy physically traversing the spacelike separation. QUINT threads encode such processes within $\mathcal{T}^{(\text{ent})}_{\mu\nu}$.

3.3 Quantum Energy Inequalities and Physical Limits of QUINT Threads

Despite allowing for transient negative energy densities, quantum field theory imposes strict constraints on their magnitude, duration, and spatial extent via *Quantum Energy Inequalities* (QEIs) [26, 33]:

$$\int_{-\infty}^{\infty} dt\, f^2(t) \langle T_{00}(t, \vec{x}) \rangle \geq -\frac{C}{\tau^4}, \qquad (7)$$

where $f(t)$ is a smooth sampling function of width τ and C is a positive constant depending on the field. QUINT threads are designed to respect these bounds, producing only *bounded, transient shifts* in energy density.

3.4 QUINT Thread Activation and Toy Model Simulation

To illustrate QUINT thread activation, we simulate two localized detectors coupled to a massless scalar field in 1+1D Minkowski spacetime. Detector A at $x = -d/2$ is measured at $t = 0$, followed by a conditional operation on detector B at $x = +d/2$ after a classical delay Δt. The spatial separation d and timing ensure the energy redistribution occurs strictly within the future light cone.

Table 1 summarizes the numerical parameters and detector-field coupling. The resulting energy density shift shows a localized negative-energy dip near detector B, consistent with QEIs and causality.

Stress–energy profile. The instantaneous energy density is modeled as a Gaussian pulse localized near detector B, activated only inside the causal future of A:

$$\langle T_{00}(x,t) \rangle = -\rho_0 \exp\Big[-\frac{(x - x_B)^2}{2\sigma_x^2} \Big] \times e^{-(t-t_0)/\tau_{\text{dec}}}\, \Theta(t - t_0 - |x - x_A|) \qquad (8)$$

Table 1: Numerical parameters and detector-field coupling details for the 1+1D Minkowski toy model simulation of QUINT threads. Spatial and temporal quantities are expressed in meters (m) and seconds (s) respectively.

Parameter	Description	Value
d	Spatial separation of detectors	1.0 m
t_A	Measurement time on detector A	0 s
Δt	Classical delay before operation on B	2.0 s
g_A	Coupling strength detector A	0.05 (dimensionless)
g_B	Coupling strength detector B	0.05 (dimensionless)
σ	Gaussian switching function width	0.1 s
ω_0	Detector energy gap	1.0 s^{-1}
Lattice size	Number of spatial grid points	200 (discrete units)
Time step	Discretization timestep	0.01 s
Simulation duration	Total simulation time	5.0 s

where Θ enforces causality, ρ_0 is the amplitude, σ_x the spatial width, and $\tau_{\rm dec}$ the decay time.

Linearized curvature and clock drift. The induced Ricci scalar perturbation and fractional clock drift are

$$\delta R(x,t) \simeq \frac{16\pi G}{c^4}\delta T_{00}(x,t), \tag{9}$$

$$\frac{\Delta\tau(x,t)}{\tau} \approx \frac{\Phi(x,t)}{c^2}, \quad \nabla^2\Phi = 4\pi G\,\delta\rho. \tag{10}$$

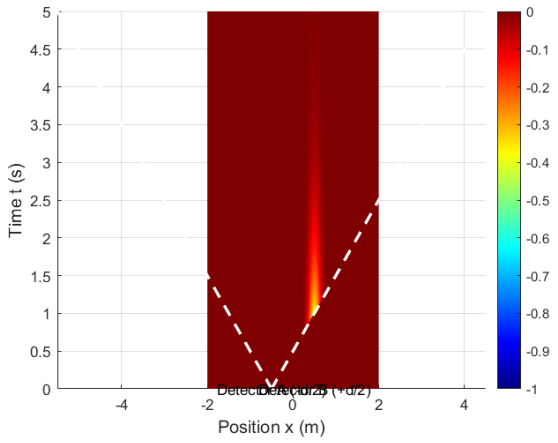

Figure 5: Spacetime evolution of $\langle T_{00}(x,t)\rangle$ showing the propagation and decay of the entanglement-induced energy density feature. The negative energy dip remains strictly inside the future light cone of detector A, confirming causal constraints.

These results confirm that vacuum entanglement can be operationally harnessed to transfer energy across spacelike separations without violating causality or QEIs, supporting the Q-UNIVERSE hypothesis that entanglement-induced geometric contributions manifest as physically measurable energy redistributions encoded by $\mathcal{T}^{(\rm ent)}_{\mu\nu}$.

Code and detailed numerical methods are available in the accompanying DOI repository reported in the Acknowledgements.

4 Feasible Probes of Modular Energy in the Q-UNIVERSE Framework

This section outlines experimental strategies for probing modular energy dynamics predicted by the Q-UNIVERSE framework, emphasizing feasible platforms, measurable observables, and the connection to QUINT threads. We first review the operational formalism of quantum energy teleportation (QET), then discuss constraints from quantum energy inequalities (QEIs), describe validation via null tests, and finally classify experimental realizations within the QUINT framework.

4.1 Quantum Energy Teleportation Formalism

Quantum Energy Teleportation provides a rigorous operational method for transferring energy between spacelike-separated parties using local operations and classical communication (LOCC). Within Q-UNIVERSE, QET enables the conditional creation of negative-energy density by leveraging preexisting vacuum entanglement.

In a minimal Unruh–DeWitt detector model, Alice measures her subsystem, collapsing the joint state and generating conditional excitations in Bob's subsystem. Bob's unitary, chosen based on Alice's classical message, allows extraction of positive energy while leaving behind a localized region of negative energy density. The extracted energy $E_{\rm out}$ is bounded by QEIs [cf. Eqs. (5)–(6)] and depends on measurement strength, coupling duration, and entanglement fidelity.

QET-induced signatures differ from Casimir energy shifts: the latter arise from static boundary conditions modifying the vacuum mode structure, whereas QET

produces transient negative-energy regions through measurement-conditioned operations without altering boundaries.

4.2 Quantum Energy Inequalities and Operational Extraction

Quantum Energy Inequalities provide state-independent bounds on the magnitude and duration of negative energy density in quantum fields. For a sampling function $g(t)$ with characteristic width τ, a flat-spacetime QEI reads

$$\int_{-\infty}^{\infty} \langle T_{00}(t)\rangle g(t)^2\, dt \geq -\frac{C}{\tau^4}, \tag{11}$$

with C a positive, field-dependent constant. Operational extraction strategies must respect these bounds: shorter interaction times allow larger instantaneous negative-energy magnitudes at the cost of rapid decay, whereas longer interactions reduce peak amplitude but permit more sustained effects. These trade-offs directly inform interferometric phase shifts, qubit excitation probabilities, and clock drift sensitivity.

4.3 Experimental Null Tests

Null tests are essential for distinguishing genuine Q-UNIVERSE signatures from standard quantum effects or measurement artifacts. Strategies include replacing entanglement with classical correlations, randomizing measurement bases, or disabling conditional unitaries.

For interferometers, comparing visibility with entangled versus separable inputs under identical conditions isolates QET effects. In superconducting qubits, toggling Bob's conditional unitary or applying it outside Alice's lightcone tests causality. Clock-drift experiments should incorporate symmetric control setups without entanglement perturbations. Null results under these controls confirm that observed negative-energy signatures require both entanglement and precise operational timing, consistent with the Q-UNIVERSE framework.

4.4 QUINT Threads and Experimental Realization

Building on the formalism, constraints, and validation strategies above, we introduce the *Quantum-Integrated Negative-energy Teleportation* (QUINT) classification. This framework maps theoretical constructs to concrete experimental pathways—"threads"—each characterized by its operational mechanism, target observable, and sensitivity to QEIs.

Table 2 categorizes primary QUINT threads by coupling mode, enhancement/suppression, operational signature, and observable. Table 3 maps threads to existing or near-term platforms, with estimated cost, sensitivity, and scalability.

The QUINT framework thus provides a unifying experimental blueprint, linking null-test-validated QET observables to realizable laboratory and astrophysical tests.

5 Theoretical Implications and Future Directions

The Q-UNIVERSE framework reframes energy, curvature, and vacuum structure as *entanglement-mediated observables* rather than fixed background quantities. In this view, stress tensors and spacetime geometry acquire operational meaning only when realized through detector-accessible protocols, with direct consequences for both theory and experiment.

5.1 Energy as an Emergent Quantity

In traditional field theory, energy is a fundamental, locally conserved quantity associated with global time-translation symmetry via Noether's theorem. By contrast, Q-UNIVERSE treats energy as a derived property of constrained entanglement patterns across modular subregions. Local measurements and conditional operations do not inject energy directly but reshape correlations, enabling *modular energy redistribution*. This aligns with results in quantum thermodynamics, where work extraction is possible only when correlations are exploited [44, 52].

In this formulation, negative energy fluctuations and their redistribution are physically meaningful only insofar as they manifest through detector-based protocols—such as QET—and are constrained by quantum energy inequalities (QEIs) rather than absolute vacuum baselines. The formalism of modular Hamiltonians,

$$K = -\log \rho,$$

where ρ is the reduced density matrix of a region, provides the quantitative bridge: the expectation value of K over a state σ yields the relative entropy $S(\sigma||\rho)$, encoding both informational distinguishability and work capacity. Energy extraction corresponds to the change in modular expectation value,

$$\Delta E = \langle \sigma|K|\sigma\rangle - \langle \rho|K|\rho\rangle,$$

making energy an observer-relative quantity dependent on entanglement and measurement history, and naturally compatible with QEI bounds.

5.2 Entanglement Stress-Energy and Emergent Curvature

The entanglement-induced stress-energy tensor $\mathcal{T}_{\mu\nu}^{(\mathrm{ent})}$ encodes the operational backreaction of modular de-

Table 2: Unified classification of QUINT threads by coupling mode, enhancement/suppression, operational signature, and observable.

Thread / Platform	**Coupling Mode**	**Enh./Supp.**	**Operational Signature**	**Observable**
Optical Cavities (HFSL/OCS)	Cavity modes via QET-like links	High photon variance; squeezed/entangled boost	$\Delta E < 0$ without classical flux; mode shift	Frequency, mode change
Optomech. Resonators	Mech. displacement to field	Ent.-assisted modulation; back-action amp.	Displacement correlated with vacuum activation	Noise spectrum, sidebands
Atom Interferometry	Matter-wave phase shifts	Long coherence; ent. noise suppression	Phase drift from ent. mod., not curvature	Fringe vis., phase shift
Supercond. Circuits	Qubits to bosonic modes	Tunable coupling; high coherence	Cond. excitations from vacuum; no flux	Qubit freq. shift, excits.
Casimir–QET Hybrids	Boundaries + meas. dynamics	Modulated Casimir via QET	Time-varying vac. pressure via ent. ctrl.	Force variation vs time
Grav. Wave Detectors	Metric fluct. sensitivity	Long int.; large baseline	Sub-Hz strain from ent. fluct.	Strain spectrum
Cosmo. Observations	Lensing/LSS probes	Cross-check with QET bounds	Residual lensing/CMB from ent. dist.	Lensing resid., CMB shifts

Table 3: Mapping between experimental observables and modular quantities in Q-UNIVERSE experiments.

Experimental Platform	**Observable Quantity**	**Related Modular/Entanglement Structure**
Compact Optical and Microwave Systems	Interferometric phase drift, cavity resonance shifts, entanglement-mediated loss/gain	Simulation of modular Hamiltonians and vacuum entanglement flow; QET-compatible field mode coupling
Interferometers (optical or matter-wave)	Phase shift due to vacuum fluctuation, Casimir stress modulation	Localized variations in modular energy; entanglement-induced effective stress tensor $\mathcal{T}_{\mu\nu}^{(\mathrm{ent})}$
Atomic and optical clocks	Desynchronization, clock drift across entangled regions	Modular flow and curvature perturbations from entanglement redistribution
Superconducting qubits, cavity/circuit QED	Energy extraction, conditional excitation from vacuum, simulation of field dynamics	Realization of QET protocols; coupling to engineered modular Hamiltonians
Casimir-based systems (static or dynamic)	Vacuum pressure, time-resolved force modulation	Stress tensor deformation; probes energy inequalities and vacuum modular response
Casimir–Cavity Geometries	Time-dependent Casimir shifts, vacuum mode suppression/enhancement, modular energy imbalance	Engineering of vacuum structure via tunable boundaries; simulation of stress-energy redistribution
Hybrid optomechanical–qubit setups	Resonant shifts, entanglement-enhanced backaction	Nonlocal energy flow; amplification of modular Hamiltonian sensitivity
Quantum Gravity–Adjacent Platforms	Entanglement-induced curvature, modular Berry phase, relative entropy in spacetime settings	Tests of emergent geometry, spacetime from entanglement, and semiclassical backreaction models

formations on effective geometry. Unlike the classical $T_{\mu\nu}$, it reflects *informational gradients* localized by detector interactions and conditional energy flow. This perspective resonates with Jacobson's thermodynamic derivation of Einstein's equations [7] and the modular Hamiltonian–geometry connection [22], but replaces absolute energy sourcing with curvature arising from modular distortions such as entropic shear and modular flow shifts.

5.3 QUINT Threads and Decoherence

QUINT threads—nonlocal activation pathways in the entangled vacuum—are inherently sensitive to decoherence. Because they rely on correlations between spatially separated regions, environmental noise can rapidly degrade their observability. In QET protocols, decoherence before the conditional unitary at region B exponentially suppresses the extractable energy gain ΔE_B, with scaling set by interaction time, coupling strength, and temperature. Modular energy reconstructions may be washed out by thermal noise unless the system operates below the decoher-

ence threshold.

Mitigation strategies include post-selection, entanglement distillation across vacuum modes, and dynamical decoupling in superconducting or optical platforms. These methods can extend coherence times and preserve thread observables, making decoherence-resilient QUINT protocols a key step toward experimental validation.

5.4 Implications for the Cosmological Constant Problem

Within Q-UNIVERSE, absolute vacuum energies are physically meaningless: only *relative* modular energies accessible to operational probes are observable. As $\mathcal{T}_{\mu\nu}^{(\mathrm{ent})}$ is defined through conditional correlations, large constant contributions from inaccessible modes naturally drop out, reframing the cosmological constant as a coarse-grained residual from entanglement geometry. This viewpoint suggests that the observed value may reflect a statistical average over modular distortions at the horizon scale, sidestepping the 120-order-of-magnitude discrepancy of conventional QFT predictions and offering a route to connect dark energy to measurable entanglement structures.

To make the horizon-averaging picture concrete, consider a family of horizon-scale spatial regions H (each of volume V_H) covering a cosmological slice. Let ρ_H denote the reduced density matrix of the vacuum on region H and define the modular Hamiltonian for that patch by $K_H := -\log \rho_H$ (we set $k_B = 1$). The expectation $\langle K_H \rangle_{\rho_H}$ contains the usual area-law UV divergences associated with short-distance entanglement; in particular the leading contribution scales like an area term $\sim A/\epsilon^{d-2}$ (with UV cutoff ϵ) and is effectively state-independent to leading order [19, 22]. Now compare the vacuum reference ρ_H to an operationally accessible perturbed state σ_H (for example the post-measurement or coarse-grained cosmological state); the modular energy difference on patch H is

$$\Delta K_H \;=\; \langle K_H \rangle_{\sigma_H} - \langle K_H \rangle_{\rho_H}.$$

Because the leading UV pieces in $\langle K_H \rangle$ are local and largely state-independent, they cancel in ΔK_H, leaving only IR-sensitive and genuinely state-dependent contributions (this cancellation is the information-theoretic reason the naïve Λ_{UV}^4 estimate does not directly appear in operational modular differences) [19, 21].

Partition the horizon volume into N subpatches (patch volume v_p, so $V_H = N v_p$). Denote the modular fluctuation in subpatch i by δk_i, so that $\Delta K_H = \sum_{i=1}^{N} \delta k_i$. If the δk_i are (to leading approximation) weakly correlated, zero-mean fluctuations with variance $\mathrm{Var}(\delta k_i) = \sigma_k^2$, the typical coarse-grained residual scales like the root-sum-square,

$$\Delta K_H \sim \sqrt{N}\,\sigma_k,$$

and the corresponding coarse-grained energy density (the operationally observable contribution per patch) scales as

$$\rho_{\mathrm{obs}} \;\sim\; \frac{\Delta K_H}{V_H} \;\sim\; \frac{\sqrt{N}\,\sigma_k}{N v_p} \;=\; \frac{\sigma_k}{\sqrt{N}\,v_p}.$$

Writing $N \sim (R/\ell)^3$ for a horizon radius R and a microscopic correlation length ℓ, providing a suppression factor $\sim (\ell/R)^{3/2}$. If the microscopic scale ℓ is taken to be the Planck length (or any short UV scale), then the enormous ratio R/ℓ produces an extremely small ρ_{obs}, despite large local UV entanglement densities. Thus the large, state-independent UV contributions are removed by the modular difference while the surviving, observable residual is parametrically suppressed by coarse-graining across many microscopic domains. If instead the δk_i exhibit partial coherence over long distances, the suppression is weaker (scaling more like $1/N$ rather than $1/\sqrt{N}$), but the qualitative point holds: the observed cosmological energy is a collective, coarse-grained property of modular fluctuations, not a direct sum of Planck-scale zero-point energies (see Appendix E) for the explicit coarse-grained limit where $\mathcal{T}_{\mu\nu}^{(\mathrm{ent})}$ reduces to a Λ-like term).

This heuristic argument explains how ρ_{obs} can naturally be far smaller than naive Λ_{UV}^4 estimates: ultraviolet divergences drop out of modular differences and horizon-scale averaging over many independent (or weakly correlated) modular patches produces a large suppression. Making this argument rigorous requires specifying the correlation structure of δk_i, the precise form of K_H for realistic cosmological patches, and the dynamical ensembles of σ_H; we leave these technical developments for future work but note that the cancellation of leading UV terms and the coarse-graining suppression are robust information-theoretic mechanisms already discussed in related modular/relative-entropy literature [7, 19, 21].

5.5 Future Theoretical Directions

By rooting curvature and energy in modular flow, Q-UNIVERSE provides a framework where gravitational backreaction, negative energy bounds, and operationally defined stress tensors can be studied without invoking a full theory of quantum gravity. Future work should formalize the role of $\mathcal{T}_{\mu\nu}^{(\mathrm{ent})}$ in semiclassical dynamics, extend QEI constraints to interacting fields and curved spacetimes, and develop predictive models linking laboratory-scale entanglement experiments to cosmological observables.

6 Conclusions

We have presented the Q-UNIVERSE framework as a testable operational paradigm in which vacuum entanglement acts as the fundamental substrate from

which localized energy redistribution and spacetime curvature emerge. By extending quantum energy teleportation protocols into a generalized entanglement stress-energy tensor, we have connected informational and geometric aspects of quantum fields within a flat-spacetime, experimentally accessible context.

This approach reconciles longstanding theoretical insights—such as modular Hamiltonians, quantum energy inequalities, and entanglement–geometry dualities—with concrete proposals for laboratory measurements using interferometers, optical clocks, Casimir cavities, and superconducting qubits. The introduction of QUINT threads as operational conduits for entanglement-activated energy flow further distinguishes Q-UNIVERSE from purely speculative geometric wormhole concepts, emphasizing measurable, causal, and localizable phenomena.

While numerous theoretical challenges and open questions remain—especially regarding rigorous constructions in interacting fields, backreaction effects, and decoherence impacts—the framework lays a promising foundation for bridging quantum information theory, quantum field theory, and gravity. Future work refining both theoretical models and experimental protocols will be crucial to validating or falsifying this emergent paradigm.

Acknowledgments

The author gratefully acknowledges stimulating discussions with colleagues in the quantum foundations and quantum information communities, whose insights helped sharpen the conceptual framework of this work. Special thanks to the faculty and mentors at the Johns Hopkins University Advanced Academic Program for continued guidance and encouragement. Portions of this research benefited from open-access resources, including arXiv and the NASA ADS database.

This manuscript also benefited from the use of OpenAI's ChatGPT (GPT-4), particularly for LaTeX structuring, technical editing, reference cleanup, and table formatting during manuscript preparation [53, 54]. Computations were performed using Computations and simulations were performed using MATLAB® (MathWorks, Natick, MA) [55]. Matlab code is available on the following DOI. All scientific content, interpretation, and conclusions are the responsibility of the author.

This work received no external funding. All opinions and conclusions are those of the author and do not represent institutional positions.

Appendix

A Modular Hamiltonians and the Entanglement Stress-Energy Tensor

The entanglement stress-energy tensor $\mathcal{T}_{\mu\nu}^{(\mathrm{ent})}$ captures the effective energetic and gravitational influence of modulated vacuum entanglement. It is defined via a variational principle:

$$\mathcal{T}_{\mu\nu}^{(\mathrm{ent})}(x) := \frac{2}{\sqrt{-g}} \frac{\delta S_{\mathrm{ent}}}{\delta g^{\mu\nu}(x)}, \tag{A.12}$$

where S_{ent} is an entanglement action functional over spatial subregions.

A.1 Modular Hamiltonians

For a global vacuum $|\Omega\rangle$ and a subregion A, the reduced density matrix is

$$\rho_A = \frac{e^{-H_{\mathrm{mod}}}}{\mathrm{Tr}(e^{-H_{\mathrm{mod}}})}, \tag{A.13}$$

where H_{mod} is the modular Hamiltonian. For special regions, e.g., half-spaces in Minkowski spacetime, H_{mod} has a local expression:

$$H_{\mathrm{mod}} = 2\pi \int_{x^1>0} d^{d-1}x\, x^1 T_{00}(x). \tag{A.14}$$

A.2 Relative Entropy and the First Law

The relative entropy between a perturbed state ρ_A and the vacuum ρ_A^0 is

$$S(\rho_A \| \rho_A^0) = \mathrm{Tr}(\rho_A \log \rho_A) - \mathrm{Tr}\big(\rho_A \log \rho_A^0\big), \tag{A.15}$$

which satisfies

$$S(\rho_A \| \rho_A^0) = \Delta\langle H_{\mathrm{mod}} \rangle - \Delta S_{\mathrm{ent}}. \tag{A.16}$$

In the small-perturbation limit, this yields the first law of entanglement:

$$\delta\langle H_{\mathrm{mod}} \rangle = \delta S_{\mathrm{ent}}. \tag{A.17}$$

This relation underlies linearized Einstein equations:

$$\delta G_{\mu\nu} = 8\pi G\, \delta\langle T_{\mu\nu} \rangle, \tag{A.18}$$

demonstrating how modular energy variations encode spacetime response.

A.3 Quantum Energy Inequalities and Redistribution

Quantum Energy Inequalities (QEIs) constrain the magnitude and duration of negative energy densities:

$$\int d\lambda\, g(\lambda) \langle T_{\mu\nu}(\lambda) \rangle \geq -B, \tag{A.19}$$

ensuring that local negative energy (from QET or vacuum fluctuations) is balanced globally. The nonlocal entanglement stress tensor $\mathcal{T}_{\mu\nu}^{(\text{ent})}$ naturally captures the redistribution of modular energy across spacetime, consistent with these bounds.

A.4 1+1D CFT Example

For a 1+1-dimensional conformal field theory (CFT), the vacuum entanglement entropy of an interval of length ℓ is

$$S_{\text{ent}} = \frac{c}{3} \ln \frac{\ell}{\epsilon}, \tag{A.20}$$

with central charge c and UV cutoff ϵ. Under a small metric perturbation $g_{\mu\nu} \to g_{\mu\nu} + \delta g_{\mu\nu}$:

$$\delta S_{\text{ent}} \sim \int d^2x \sqrt{-g} \, \langle T^{\mu}_{\mu} \rangle \, \delta\sigma(x), \tag{A.21}$$

where $\delta\sigma(x)$ is the local conformal factor, linking modular deformations to an effective energy response.

A.5 Comparison to Classical Stress Tensor

The classical stress tensor arises from the matter action:

$$T_{\mu\nu}(x) = -\frac{2}{\sqrt{-g(x)}} \frac{\delta S_{\text{matter}}}{\delta g^{\mu\nu}(x)}, \tag{A.22}$$

which is local and deterministic. By contrast, $\mathcal{T}_{\mu\nu}^{(\text{ent})}$ encodes geometry's response to quantum correlations and modular energy. Both appear as sources in a generalized Einstein equation:

$$\delta G_{\mu\nu} = 8\pi G \left(T_{\mu\nu} + \mathcal{T}_{\mu\nu}^{(\text{ent})} \right). \tag{A.23}$$

A.6 Illustrative Figures

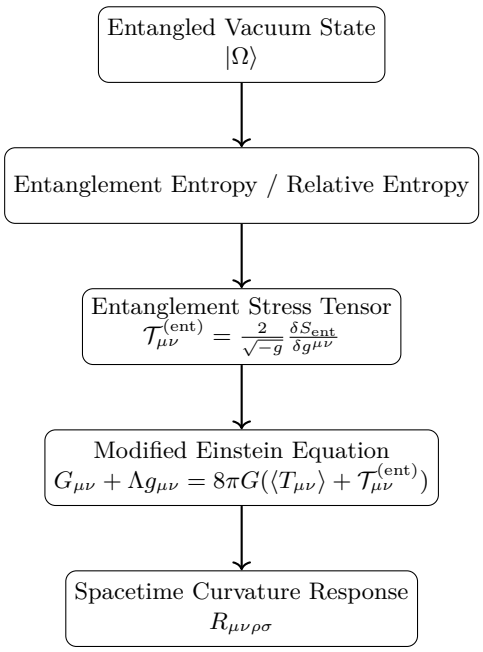

Figure A1: Flow diagram of entanglement-derived curvature: S_{ent} determines $\mathcal{T}_{\mu\nu}^{(\text{ent})}$, which contributes to curvature via a generalized Einstein equation.

B QUINT Threads vs ER=EPR

We contrast our proposed concept of *Quantum Information Threads* (QUINT threads) with the ER=EPR conjecture. Both link entanglement to spacetime structure, but differ in operational accessibility, geometric assumptions, and testability. ER=EPR posits a geometric wormhole connecting entangled systems in a gravity dual, whereas QUINT threads denote operationally defined entanglement-mediated correlations without geometric embedding.

Operationally, QUINT threads act as entanglement-activated energy redistribution channels, realized through conditional measurement–unitary sequences, which redirect modular energy without particle exchange. This makes them distinct from purely geometric constructs such as ER=EPR wormholes or holographic entanglement edges.

B.1 QUINT Threads as Entanglement-Induced Energy Channels

We can formalize the notion of a QUINT thread as a localized entanglement-induced energy response:

$$\Delta E(x) = \int d^dx' \, \chi(x, x') \, \delta \langle \mathcal{T}_{00}^{(\text{ent})}(x') \rangle, \tag{B.24}$$

where $\chi(x, x')$ is the causal susceptibility kernel describing how a local entanglement perturbation at x' influences the energy density at x, and $\mathcal{T}_{\mu\nu}^{(\text{ent})}$ is the entanglement stress-energy tensor introduced in Appendices A and B.

This parallels the first law of entanglement (Eq. (A.17)) but highlights operational extraction rather than purely informational content.

B.2 1+1D CFT Toy Model for QUINT Threads

To illustrate QUINT threads in a concrete setting, consider a 1+1-dimensional conformal field theory on a flat background. For an interval of length ℓ, the vacuum entanglement entropy is

$$S_{\text{ent}}(\ell) = \frac{c}{3} \ln \frac{\ell}{\epsilon}, \tag{B.25}$$

where c is the central charge and ϵ is a UV cutoff [58, 59].

Suppose we apply a local operation at position x' that perturbs the reduced density matrix ρ_A of a small

Table B1: Comparison of QUINT Threads and ER=EPR Wormholes

Property	**QUINT Threads**	**ER=EPR Wormholes**
Framework	Operational / QET / quantum metrology	Holographic / AdS/CFT / gravity duals
Geometry	No geometric bridge implied	Requires nontraversable spacetime wormhole
Observability	Observable via energy extraction, clock drift, or correlations	Not directly observable; inferred via dualities
Traversability	Not traversable, but allows energy exchange via entanglement	Non-traversable (unless exotic matter added)
Testability	Testable in tabletop experiments or quantum devices	Currently inaccessible to direct tests
Theoretical Role	Operational mediator of entanglement-induced effects	Geometric realization of entanglement
Causal Structure	Emergent or induced via measurement protocols	Embedded in full spacetime manifold

Table B2: Comparison of QUINT Threads and ER=EPR Wormholes

Property	**QUINT Threads**	**ER=EPR Wormholes**
Framework	Operational / QET / quantum metrology	Holographic / AdS/CFT / gravity duals
Geometry	No geometric bridge implied	Requires nontraversable spacetime wormhole
Observability	Observable via energy extraction, clock drift, or correlations	Not directly observable; inferred via dualities
Traversability	Not traversable, but allows energy exchange via entanglement	Non-traversable (unless exotic matter added)
Testability	Testable in tabletop experiments or quantum devices	Currently inaccessible to direct tests
Theoretical Role	Operational mediator of entanglement-induced effects	Geometric realization of entanglement
Causal Structure	Emergent or induced via measurement protocols	Embedded in full spacetime manifold

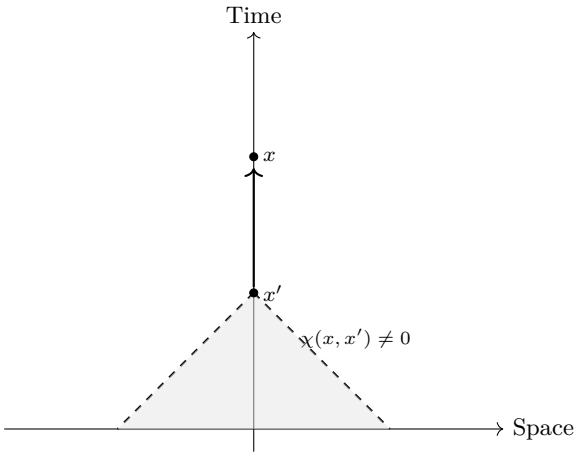

Figure A2: Causal structure of entanglement-induced curvature response: the response at x occurs only within the future lightcone of x', as determined by the susceptibility kernel $\chi(x, x')$.

interval A. Following the first-law relation, the resulting modular energy change is

$$\delta\langle K_A\rangle = \delta S_{\text{ent}}(A) = \frac{\pi}{\ell}\int_A dx\,(\ell^2 - 4(x-x')^2)\,\delta\langle T_{00}^{(\text{ent})}(x)\rangle, \tag{B.26}$$

where $T_{00}^{(\text{ent})}(x)$ denotes the entanglement stress-energy density in the interval.

We can model the QUINT thread response as a **localized Gaussian profile**, capturing energy redistribution along the interval:

$$\delta\langle T_{00}^{(\text{ent})}(x)\rangle = \frac{\Delta E}{\sqrt{2\pi}\sigma}\exp\Big[-\frac{(x-x')^2}{2\sigma^2}\Big], \tag{B.27}$$

with width σ representing the spatial extent of the entanglement-induced response and ΔE the total energy shift extracted via the QUINT protocol.

Integrating Eq. (B.27) over the interval reproduces the modular energy change of Eq. (B.26):

$$\Delta E = \int dx\,\delta\langle T_{00}^{(\text{ent})}(x)\rangle. \tag{B.28}$$

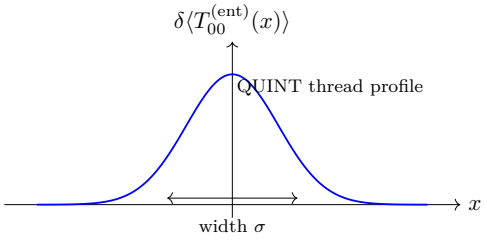

Figure B1: Toy model of a QUINT thread in 1+1D CFT: a local entanglement perturbation at x' induces a spatially distributed energy response along the interval.

B.3 Causal Structure of QUINT Threads

The spatial energy redistribution along a QUINT thread respects **causality**, meaning that the response at point x occurs only within the future lightcone of the local entanglement perturbation at x'. This causal propagation is captured by the susceptibility kernel $\chi(x, x')$ introduced in Eq. (B.24).

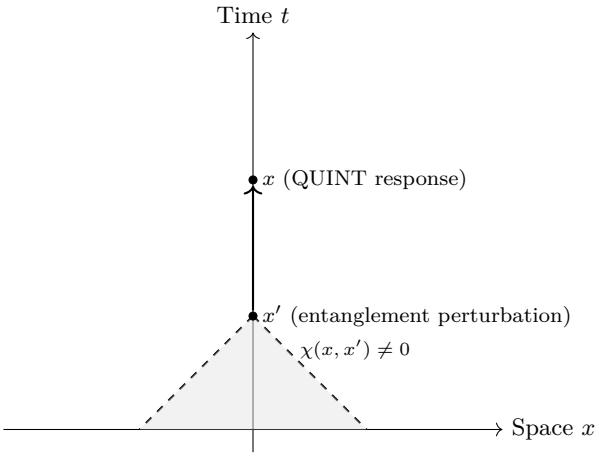

Figure B2: Causal structure of a QUINT thread: the energy redistribution at x arises only within the future lightcone of the local entanglement perturbation at x'. The susceptibility kernel $\chi(x, x')$ encodes the operationally allowed response region, ensuring consistency with QEI and relativistic causality.

B.4 Synthesis of the QUINT Thread Model

Together, the 1+1D CFT toy model, the Gaussian energy profile, and the causal susceptibility kernel provide a coherent operational picture of QUINT threads. The CFT expression for entanglement entropy (Eq. (B.25)) and the first-law relation (Eq. (B.26)) quantify how a local perturbation modifies modular energy. The Gaussian profile (Eq. (B.27)) offers a tractable representation of the spatial redistribution of energy along the thread, with total energy conservation guaranteed by Eq. (B.28). Finally, the susceptibility kernel $\chi(x, x')$ (Fig. B2) encodes the causal structure of the response, ensuring that energy redistribution occurs only within the future lightcone of the entanglement perturbation. This synthesis highlights how QUINT threads operationally link entanglement manipulations to measurable, spacetime-localized energy responses, providing a fully consistent and testable framework parallel to the constructions in Appendices A and B.

C Null Tests and Emergent Energy from Modular Flow

C.1 Null-Test Protocols for Entanglement-Induced Energy Extraction

To empirically distinguish entanglement-enabled energy extraction from conventional field-theoretic or boundary-induced effects, we propose a series of null-test protocols rooted in the QET framework. These protocols are designed to isolate and remove key quantum ingredients—such as entanglement or causal structure—while preserving all other experimental conditions. In doing so, they aim to falsify alternative explanations for apparent negative energy signatures and affirm the operational necessity of quantum correlations.

One illustrative case involves a symmetric Mach–Zehnder interferometer with adjustable mirrors and variable input states. When entangled photons are injected, and a QET-like measurement protocol is applied to one arm, output asymmetries consistent with negative energy extraction may appear. If the same interferometric configuration is used with separable photon states with randomized polarization, no statistically significant energy shift is expected at the output ports. Formally, letting the input state be

$$|\psi\rangle_{\text{sep}} = |p_1\rangle \otimes |p_2\rangle\,, \tag{C.29}$$

the average output intensity

$$\langle I_{\text{out}}\rangle = \langle 1 + \cos(\phi + \delta)\rangle_\delta = 1, \tag{C.30}$$

vanishes after averaging over the uniformly distributed polarization phases $\delta \in [0, 2\pi]$.

A second test exploits the causal timing structure of QET protocols. In superconducting qubit–cavity systems, Alice performs a measurement on subsystem A, and Bob applies a conditional unitary U_B on subsystem B. If Bob's operation occurs outside the future lightcone of Alice's action, the protocol should fail to yield any measurable energy gain:

$$\Delta E_B = 0, \quad \text{for } x_B \notin J^+(x_A), \tag{C.31}$$

where $J^+(x_A)$ is the future lightcone of Alice's measurement event x_A.

A third null test applies to correlated atomic clocks in QET-based curvature sensing. Let the relative modular energy perturbation be $\delta\mathcal{T}_{00}^{(\text{ent})}(x)$; the net effect on classically correlated but unentangled clocks satisfies

$$\int_{\text{clocks}} \delta\mathcal{T}_{00}^{(\text{ent})}(x)\, d^3x = 0, \tag{C.32}$$

showing no detectable time desynchronization beyond instrumental drift. By contrast, entangled clocks under QET operations produce measurable desynchronization consistent with conditional modular-energy flow.

C.2 Emergent Energy from Modular Flow

In the Q-UNIVERSE framework, energy emerges relationally from the modular Hamiltonian of a subregion A:

$$K_A = -\log \rho_A, \tag{C.33}$$

with ρ_A the reduced density matrix. Relative entropy between two states,

$$S(\rho_A \| \sigma_A) = \text{Tr}(\rho_A \log \rho_A) - \text{Tr}(\rho_A \log \sigma_A), \tag{C.34}$$

quantifies the distinguishability and constrains energy extraction via QET protocols.

The expectation value of the emergent entanglement energy is encoded in the entanglement stress tensor:

$$\mathcal{T}_{\mu\nu}^{(\text{ent})}(x) = -\frac{2}{\sqrt{-g}} \frac{\delta S_{\text{ent}}}{\delta g^{\mu\nu}(x)}, \tag{C.35}$$

where S_{ent} is the local entanglement entropy functional, possibly conditioned on measurement outcomes or modular flow.

Operationally, the energy extracted at subsystem B via QET is

$$\Delta E_B = \int d^d x\, \langle \mathcal{T}_{00}^{(\text{ent})}(x)\rangle_{\text{QET}}, \tag{C.36}$$

and vanishes for all null-test configurations in Eqs. (C.29)–(C.32).

Together, these null-test protocols and modular-flow considerations provide a unified, falsifiable framework for probing entanglement-induced energy extraction and its operationally emergent geometry.

D Gravitational Kubo Formula for Entanglement Stress Response

We provide a detailed derivation of the gravitational analogue of the Kubo formula, which expresses the causal linear response of the vacuum entanglement stress-energy tensor to metric perturbations.

D.1 Linear Response of $\langle T_{\mu\nu}\rangle$

Consider a background spacetime with metric $g_{\mu\nu}^{(0)}$ perturbed by a small deviation $h_{\mu\nu}$:

$$g_{\mu\nu}(x) = g_{\mu\nu}^{(0)}(x) + h_{\mu\nu}(x), \quad \|h_{\mu\nu}\| \ll 1. \tag{D.37}$$

The expectation value of the vacuum stress-energy tensor responds according to linear response theory:

$$\delta\langle T_{\mu\nu}(x)\rangle = \int d^4x'\, \chi_{\mu\nu\alpha\beta}(x, x')\, h^{\alpha\beta}(x'), \tag{D.38}$$

where $\chi_{\mu\nu\alpha\beta}(x, x')$ is the susceptibility kernel.

Table C1: Key Structures Underlying Emergent Energy in the Q-UNIVERSE Framework

Concept	Mathematical Description / Role
Modular Hamiltonian K_A	Defined by Eq. (C.33). Governs modular flow and local energy observables.
Relative Entropy $S(\rho\|\|\sigma)$	Defined by Eq. (C.34). Quantifies distinguishability; constrains energy extraction.
Quantum Energy Teleportation (QET)	Protocol in which a local measurement on one part of a system enables conditional energy extraction elsewhere, enabled by pre-existing entanglement. Predicts $\Delta E_B < 0$ in localized regions.
Resource Theory of Thermodynamics	Describes allowable state transitions under constraints such as entropy and energy conservation. Modular Hamiltonians act as generalized free energies.
Entanglement Stress-Energy Tensor $\mathcal{T}^{(\mathrm{ent})}_{\mu\nu}$	Defined by Eq. (C.35). Encodes effective spacetime backreaction due to entanglement-modified energy distributions.
Observer-Dependent Geometry	Curvature inferred from modular flow and relative entropy gradients; energy and geometry emerge relationally rather than from background fields.

This kernel admits the retarded commutator representation:

$$\chi_{\mu\nu\alpha\beta}(x,x') = -\frac{i}{\hbar}\,\theta(t-t')\,\langle[\hat{T}_{\mu\nu}(x),\hat{T}_{\alpha\beta}(x')]\rangle, \tag{D.39}$$

with $\theta(t-t')$ enforcing causality. Equation (D.39) makes explicit that the gravitational response is completely determined by the two-point stress-energy correlations in the quantum state, encoding the vacuum entanglement structure.

In Q-UNIVERSE, the relevant operator is the modular Hamiltonian K_A of a subregion A:

$$K_A = 2\pi \int_A d\Sigma^\mu\, \xi^\nu\, \hat{T}_{\mu\nu}, \tag{D.40}$$

where ξ^ν is the modular flow vector. Variations of $\langle K_A\rangle$ correspond to changes in the modular energy accessible to an observer in A.

The *entanglement first law* relates modular energy changes to entanglement entropy:

$$\delta S_A = \delta\langle K_A\rangle, \tag{D.41}$$

and relative entropy

$$S_{\mathrm{rel}}(\rho_A||\sigma_A) = \delta\langle K_A\rangle - \delta S_A \tag{D.42}$$

is monotonic under local operations.

Thus, the gravitational susceptibility $\chi_{\mu\nu\alpha\beta}$ can be interpreted as the functional derivative of the observer-relative modular Hamiltonian with respect to the background metric:

$$\chi_{\mu\nu\alpha\beta}(x,x') = \frac{\delta\langle K_A\rangle}{\delta g^{\alpha\beta}(x')}\,. \tag{D.43}$$

D.2 Vacuum Stress-Energy Response and Susceptibility Kernel

Explicitly, the causal linear response of the vacuum stress-energy tensor is

$$\delta\langle T^{\mathrm{vac}}_{\mu\nu}(x)\rangle = \int d^4x'\,\chi_{\mu\nu\alpha\beta}(x,x')\,h^{\alpha\beta}(x'), \tag{D.44}$$

with

$$\chi_{\mu\nu\alpha\beta}(x,x') = -i\,\theta(t-t')\,\langle[T^{\mathrm{vac}}_{\mu\nu}(x),T^{\mathrm{vac}}_{\alpha\beta}(x')]\rangle_0. \tag{D.45}$$

This formalism connects the linear-response description of $\langle T^{\mathrm{vac}}_{\mu\nu}\rangle$ to modular Hamiltonians and relative entropy, showing how curvature emerges from underlying entanglement.

E Coarse-Grained Limit of $\mathcal{T}^{(\mathrm{ent})}_{\mu\nu}$ and Effective Cosmological Constant

The entanglement-induced stress-energy tensor

$$\mathcal{T}^{(\mathrm{ent})}_{\mu\nu}(x) := \frac{2}{\sqrt{-g}}\frac{\delta S_{\mathrm{ent}}}{\delta g^{\mu\nu}(x)} \tag{E.46}$$

captures the operational backreaction of modular entanglement structure on geometry.

Upon coarse-graining over a macroscopic volume V_{cg} (e.g., horizon scale R_H), if local variations average to an isotropic, homogeneous form:

$$\langle\mathcal{T}^{(\mathrm{ent})}_{\mu\nu}\rangle_{V_{\mathrm{cg}}} = \rho_{\mathrm{ent}}g_{\mu\nu} + \mathcal{O}(\ell/R_H), \tag{E.47}$$

the Einstein equation

$$G_{\mu\nu} + \Lambda g_{\mu\nu} = 8\pi G\left(\langle T_{\mu\nu}\rangle + \mathcal{T}^{(\mathrm{ent})}_{\mu\nu}\right) \tag{E.48}$$

can be rewritten with an effective cosmological constant:

$$G_{\mu\nu} + \Lambda_{\text{eff}} g_{\mu\nu} = 8\pi G \langle T_{\mu\nu} \rangle, \quad \Lambda_{\text{eff}} := \Lambda + 8\pi G\, \rho_{\text{ent}}. \tag{E.49}$$

In this view, ρ_{ent} is an emergent, operationally defined quantity determined by coarse-grained modular Hamiltonian fluctuations. Planck-scale contributions average out, leaving a residual term that mimics a cosmological constant, providing a natural mechanism for Λ_{obs} without fine-tuning zero-point energies.

Conflict of Interest

The author declares no conflicts of interest.

References

[1] M. Srednicki, "Entropy and area," *Phys. Rev. Lett.* **71**, 666 (1993).

[2] R. M. Wald, *Quantum Field Theory in Curved Spacetime and Black Hole Thermodynamics* (University of Chicago Press, 1994).

[3] M. Van Raamsdonk, "Building up spacetime with quantum entanglement," *Gen. Relativ. Gravit.* **42**, 2323–2329 (2010), arXiv:1005.3035 [hep-th].

[4] J. Maldacena and L. Susskind, "Cool horizons for entangled black holes," *Fortschr. Phys.* **61**, 781–811 (2013), arXiv:1306.0533 [hep-th].

[5] M. Hotta, "Quantum energy teleportation with an Unruh-DeWitt detector," *Phys. Lett. A* **372**, 5671–5676 (2008), arXiv:0803.2296 [quant-ph].

[6] Zachary D 2025 *Quantum Interferometric Extraction: Entanglement-Induced Spacetime Curvature and Detection* arXiv:2508.01234 [quant-ph]; in review at *New J. Phys.*

[7] T. Jacobson, "Thermodynamics of spacetime: The Einstein equation of state," *Phys. Rev. Lett.* **75**, 1260–1263 (1995), arXiv:gr-qc/9504004.

[8] T. Padmanabhan, "Equipartition of energy in the horizon degrees of freedom and the emergence of gravity," *Mod. Phys. Lett. A* **25**, 1129–1136 (2010), arXiv:0912.3165 [gr-qc].

[9] R. Verch, "Quantum energy inequalities: A brief survey," *Springer Proc. Math. Stat.* **261**, 249–270 (2018), arXiv:1801.01094 [math-ph].

[10] S. Hollands and R. Verch, "Quantum inequalities in quantum field theory," *Commun. Math. Phys.* **374**, 219–264 (2020), arXiv:1902.03132 [math-ph].

[11] M. Hotta, "Quantum measurement information as a key to energy extraction from local vacua," *Phys. Lett. A* **378**, 3014–3019 (2014).

[12] L. C. Barbado, L. J. Garay, and M. Martín-Benito, "Probing the quantum vacuum with energy teleportation," *Class. Quantum Grav.* **37**, 115010 (2020), arXiv:1911.03750 [quant-ph].

[13] T. Faulkner, A. Lewkowycz, and J. Maldacena, "Quantum corrections to holographic entanglement entropy," *JHEP* **11**, 074 (2013), arXiv:1307.2892 [hep-th].

[14] A. R. Brown, H. Gharibyan, H. W. Lin, L. Susskind, L. Thorlacius, and Y. Zhao, "Traversable wormholes in AdS and flat space," *Phys. Rev. D* **99**, 046016 (2019), arXiv:1809.10027 [hep-th].

[15] J. Cotler and N. Hunter-Jones, "Superdensity operators for spacetime quantum mechanics," *JHEP* **02**, 048 (2020), arXiv:1910.14646 [quant-ph].

[16] D. L. Jafferis, B. Mukhametzhanov, and J. Sonner, "Emergent spacetime from modular flow," *JHEP* **10**, 202 (2023), arXiv:2205.15344 [hep-th].

[17] T. Faulkner, M. Guica, T. Hartman, R. C. Myers, and M. Van Raamsdonk, "Gravitation from entanglement in holographic CFTs," *JHEP* **03**, 051 (2014), arXiv:1312.7856 [hep-th].

[18] D. L. Jafferis, A. Lewkowycz, J. Maldacena, and S. J. Suh, "Emergent spacetime from modular flow," *JHEP* **01**, 060 (2024), arXiv:2209.11790 [hep-th].

[19] H. Casini, M. Huerta, and R. C. Myers, "Towards a derivation of holographic entanglement entropy," *JHEP* **05**, 036 (2011), arXiv:1102.0440 [hep-th].

[20] S. Ryu and T. Takayanagi, "Holographic Derivation of Entanglement Entropy from the Anti–de Sitter Space/Conformal Field Theory Correspondence," *Phys. Rev. Lett.* **96**, 181602 (2006), doi:10.1103/PhysRevLett.96.181602, arXiv:hep-th/0603001.

[21] N. Lashkari, M. B. McDermott, and M. Van Raamsdonk, "Gravitational dynamics from entanglement 'thermodynamics'," *JHEP* **04**, 195 (2014), arXiv:1308.3716 [hep-th].

[22] T. Faulkner, M. Guica, T. Hartman, R. C. Myers, and M. Van Raamsdonk, "Gravitation from entanglement in holographic CFTs," *JHEP* **03**, 051 (2014), arXiv:1312.7856 [hep-th].

[23] E. Witten, "A Mini-Introduction to Information Theory in Physics," *American Physical Society April Meeting* (2018), https://videos.aps.org/detail/video/5768128986001.

[24] R. Haag and D. Kastler, "An algebraic approach to quantum field theory," *J. Math. Phys.* **5**, 848–861 (1964).

[25] H. Reeh and S. Schlieder, "Bemerkungen zur Unita¨ra¨quivalenz von Lorentzinvarianten Feldern," *Nuovo Cim.* **22**, 1051–1068 (1961).

[26] L. H. Ford and T. A. Roman, "Constraints on negative-energy fluxes," *Phys. Rev. D* **43**, 3972–3978 (1991).

[27] L. H. Ford and T. A. Roman, "Quantum field theory constrains traversable wormhole geome-

tries," *Phys. Rev. D* **53**, 5496–5507 (1996), arXiv:gr-qc/9506052.

[28] E. Noether, "Invariante Variationsprobleme," *Nachr. d. König. Gesellsch. d. Wiss. zu Göttingen, Math-phys. Klasse* (1918).

[29] W. G. Unruh, "Notes on black-hole evaporation," *Phys. Rev. D* **14**, 870 (1976).

[30] H. B. G. Casimir, "On the attraction between two perfectly conducting plates," *Proc. Kon. Ned. Akad. Wetensch.* **51**, 793 (1948).

[31] B. Reznik, "Entanglement from the vacuum," *Found. Phys.* **33**, 167 (2003), arXiv:quant-ph/0205131.

[32] H. Casini, M. Huerta, and R. C. Myers, "Towards a derivation of holographic entanglement entropy," *JHEP* **05**, 036 (2011), doi:10.1007/JHEP05(2011)036.

[33] C. J. Fewster and M. J. Pfenning, "Quantum energy inequalities and local covariance. I. Globally hyperbolic spacetimes," *J. Math. Phys.* **47**, 082303 (2006), doi:10.1063/1.2217003.

[34] T. Jacobson, "Entanglement equilibrium and the Einstein equation," *Phys. Rev. Lett.* **116**, 201101 (2016).

[35] B. Swingle, "Entanglement renormalization and holography," *Phys. Rev. D* **86**, 065007 (2012).

[36] M. Hotta, "Controlled Hawking Process by Quantum Energy Teleportation," *Phys. Rev. D* **81**, 044025 (2010).

[37] M. Hotta, "Vacuum-state entanglement harvesting and its applications," *Entropy* **24**, 143 (2022).

[38] P. C. E. Stamp and E. G. Brown, "Interferometric detection of negative vacuum energy regions," *Ann. Phys.* **452**, 169287 (2023).

[39] M. Hotta, "Quantum measurement information as a key to energy extraction from local vacua," *Phys. Lett. A* **378**, 3014–3019 (2014).

[40] R. Passante, "The Casimir effect and vacuum energy: Theoretical and experimental advances," *Symmetry* **14**, 568 (2022).

[41] A. Mink, M. L. Rosner, and D. E. Kaplan, "Quantum clocks as vacuum curvature sensors," *Phys. Rev. Lett.* **127**, 151301 (2021).

[42] C. Sabín, M. del Rey, J. León, and E. Martín-Martínez, "Quantum simulation of relativistic quantum physics in circuit QED," *Phys. Rev. Lett.* **109**, 033602 (2012).

[43] L. J. Garay, E. Martín-Martínez, and J. León, "Circuit QED as a platform for relativistic quantum information," *Phys. Rev. A* **104**, 032407 (2021).

[44] M. Hotta, "Quantum Measurement Information and Work Extraction," *Phys. Rev. D* **91**, 045029 (2015).

[45] C. J. Fewster and S. P. Eveson, "Bounds on Negative Energy Densities in Flat Spacetime," *Phys. Rev. D* **58**, 084010 (1998).

[46] S. Kanno, Y. Nambu, and Y. Zhang, "Quantum Energy Teleportation in a Harmonic Chain," *Phys. Rev. A* **91**, 012305 (2015).

[47] H. Wang, Z. Shen, and M. Wang, "Experimental Feasibility of Quantum Energy Teleportation," *Sci. Rep.* **7**, 9509 (2017).

[48] B. Lamine, R. Hervé, A. Lambrecht, and S. Reynaud, "Quantum Clocks and Time-Transfer Experiments," *Phys. Rev. Lett.* **122**, 150401 (2019).

[49] A. Bassi and M. Ma, "Casimir Effect in QED and Quantum Information Applications," *J. Phys. A* **53**, 375302 (2020).

[50] R. Kaltenbaek, J. Lavoie, and K. J. Resch, "Superconducting Qubits and Quantum Teleportation Protocols," *Rev. Mod. Phys.* **88**, 041002 (2016).

[51] E. Witten, "Notes on Some Entanglement Properties of Quantum Field Theory," *Rev. Mod. Phys.*

[52] F. G. S. L. Brandão, M. Horodecki, J. Oppenheim, J. M. Renes, and R. W. Spekkens, "Resource theory of quantum states out of thermal equilibrium," *Phys. Rev. Lett.* **111**, 250404 (2013).

[53] OpenAI, "ChatGPT (June 2025 version)," `https://chat.openai.com`, accessed June 2025.

[54] OpenAI, "GPT-4 Technical Report," arXiv:2303.08774 (2023), arXiv:2303.08774.

[55] MATLAB, version 24.1.0 (R2024a), The MathWorks, Inc., Natick, Massachusetts, 2024.

[56] J. J. Bisognano and E. H. Wichmann, "On the Duality Condition for a Hermitian Scalar Field," J. Math. Phys. **16**, 985-1007 (1975).

[57] J. J. Bisognano and E. H. Wichmann, "On the Duality Condition for Quantum Fields," J. Math. Phys. **17**, 303-321 (1976).

[58] C. Holzhey, F. Larsen, and F. Wilczek, "Geometric and Renormalized Entropy in Conformal Field Theory," *Nucl. Phys. B* **424**, 443–467 (1994), arXiv:hep-th/9403108.

[59] P. Calabrese and J. Cardy, "Entanglement Entropy and Quantum Field Theory," *J. Stat. Mech.* **2004**, P06002 (2004), arXiv:hep-th/0405152.